International Journal of Theoretical & Applied Sciences **6**(1): 1-8(2014)

ISSN No. (Print): 0975-1718
ISSN No. (Online): 2249-3247

Characterization of Vibrational Modes of Neutral $(MgO)_n$(*n* = 3, 4, 6, 8, 9 and 12) Clusters

Fathi Bawa
Department of Physics,
Department of Physics, Faculty of Science, Misurata University, Libya

(Received 05 December, 2013, Accepted 25 December, 2013)

(*Corresponding author, Fathi Bawa)*

ABSTRACT: The vibrational active modes of $(MgO)_n$ (*n* = 3, 4, 6, 8, 9 and 12) stacks of squares, hexagons, octagons and sphere clusters have been investigated using density functional theory (DFT) calculations. Frequencies of modes show three different regions at or near (i) the high frequency vibrations, (ii) intermediate frequency vibrations, and (iii) the low frequency vibrations. For *n* = 3 and *n* = 4 clusters, infrared (IR) active modes were calculated at about 770 cm^{-1} and 865 cm^{-1} respectively, while for 6, 8, 9 and 12 were found between 500 and 750 cm^{-1}, and the spectra are almost dependent of cluster size. These behaviour previously observed near 16 and 22 microns [J. Chem. Phys. 116, 2400 (2002)]. In addition, vibrational assignments were compared to the experimental and theoretical infrared results. On this basis, MgO clusters are applied in industry and home and have the advantages of good transparency and high brightness to reduce solar radiation in order to protect the general public from the harmful effects of these radiations.

Keywords: Infrared modes, $(MgO)_n$ clusters, Density functional theory, IR, Optical

I. INTRODUCTION

With the rapid development of nanotechnology, magnesium oxide clusters based on metal nanostructures gain increasing demand for new photocatalytic applications due to its distinctive physical and chemical properties quite different from the discrete molecules or bulk matter [1-6]. The deeply studying of limited or unlimited clusters is kind of the respective behaviour of these materials, which lies at the heart of many technologies spanning illumination, e.g. solar energy production [7]. Over the past decade, there are many studies already been focused on the structure and stability of MgO nanoscale which exists as different structures such as the cubic structure, hexagonal and octagonal ring stacks, are formed with increasing the diameter of the cluster ring [8], and we found that the $(MgO)_3$ clusters are the most stable subunits or building blocks in alkaline earth oxides.

Nanoparticle ensembles represent strongly absorbing and scattering light. In this regard, the optical properties of bulk and MgO materials have been investigated [9, 10] for a wide area of applications. Magnesium Oxide is important in applications, due to a number of advantageous properties, for example it is used as a catalyst in chemical reactions, adsorption of pollutants, controlled release and electronic devices as data storage etc [11, 12].

Infrared is one of the more informative techniques for the characterization of adsorbed molecules as nitrite and nitrate species formed on MgO surfaces [13]. In addition, during sunshine hours, the oxide material is irradiated with infrared light with a span of different wavelengths. The material will absorb some of the light at certain wavelengths that are characteristic to its chemical composition, and then get heated and simultaneously storage the harmful radiation as well as produce bright ray emission in the range of visible light region. This can be usefulness of optical storage to protective people from the strong radiations especially in the hot climates. Moreover, it has recently been shown that MgO nanoparticles being widely used in important industrial processes, leading to control the sun radiation through window as storage media [14], which produces high transparency when the particles interact with IR rays from sunlight. The properties of MgO particularly a vibrational frequency of about 12.7 µm (785 cm^{-1}) [15], a wide optical band gap of 7.8 eV [16] with a high melting temperature point 2826°C, high ionic character and transparent media, and it is an insulating ionic simple oxide [17], make magnesia useful in the production of photocells applications as well as extensive research on the optoelectronic applications. For example, MgO ceramic has excellent thermal and optical light transmitting properties [18], which are related to the high melting point and ionic bonding. Magnesium oxide is accordingly a perfect choice for a material that would demonstrate by its spectral behaviour of the atomic vibration frequencies in clusters and to identify the active modes as well as demonstrated to be utility in nanostructure superconductors [19].

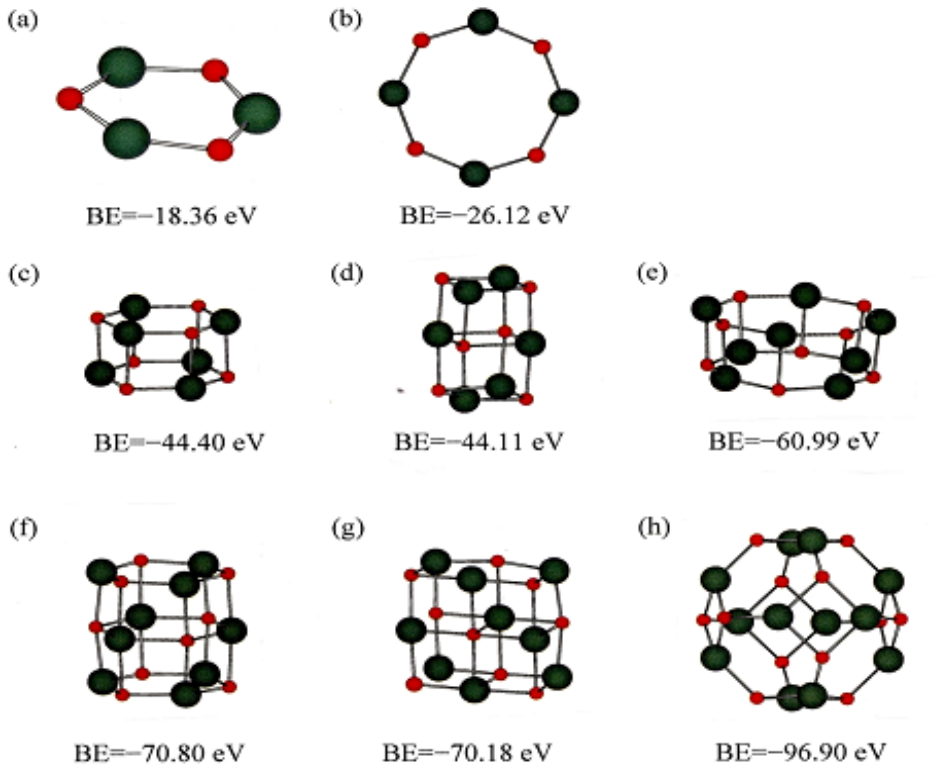

Fig. 1. The eight different cluster models of (a) Mg_3O_3 (b) Mg_4O_4 (c) Mg_6O_6 (2-hexa-ring) (d) Mg_6O_6 (slab) (e) Mg_8O_8 (2-octa-ring) (f) Mg_9O_9 (3-hexa-ring) (g) Mg_9O_9 (slab) (h) $Mg_{12}O_{12}$ (sphere), with the energies relative to the most stable clusters.

This indication of recent investigations using the density functional theory have revealed the strongest peaks on its infrared spectra, are located in the range from 650 to 750 cm^{-1} [20]. Among these, ordered magnesium oxide clusters have attracted special attention due to its possible applications in industries.

In this paper, we report our calculations on the theoretical infrared properties of the $(MgO)_n$, clusters in the size of n = 3, 4, 6, 8, 9 and 12. We have been considered $(MgO)_3$ (hexagonal ring), $(MgO)_4$ (octagonal ring), $(MgO)_6$ (2-hexagonal ring stack and slab structure), $(MgO)_8$ (2-octagonal ring stack), $(MgO)_9$ (3-hexagonal ring stack and slab structure) and $(MgO)_{12}$ (spherical structure). Fig.1. illustrates the sample optimized structures of MgO nanotube cluster. More interestingly, these clusters are found to possess Infrared-active modes, whose intensity increases with increasing cluster size. Frequencies are identified in terms of vibrational modes of two different atoms Mg and O, and include sharp features especially in the high energy region of each cluster.

II. MATERIALS AND METHOD

Depending on the size and shape of MgO clusters, the MgO has simple particle packing produces different shapes including, cubic structures, hexagonal, octagonal ring structures and sphere models with the stable (100) surface unit cells [21]. $(MgO)_6$, $(MgO)_8$ and $(MgO)_9$ clusters are stable clusters, since all are built possibly from stable four, six and eight sub-units [8]. The B3LYP [22-24] and the 6-311G(d) basis set are used in all calculations performed within Gaussian 98 package [25], to reproduce the characteristics of the $(MgO)_n$ clusters and obtain converged results for the binding energies, bond lengths and bond angles in their stable forms. The optimized structures of $(MgO)_n$ (n = 3, 4, 6, 8, 9 and 12) were taken from the results of Ref. [8]. To assure the existence of stable minima on the corresponding potential energy surface by computing the vibrational frequencies which displayed none of any imaginary frequencies. Moreover, a reliable assignment of the fundamentals for all clusters was proposed based on the calculated frequencies and corresponding intensities. Heijnsbergen *et.al.*, [26], have experimentally observed the IR frequencies of 16-22 µm are compared with our spectra calculated at the DFT level leading to structural assignments.

III. RESULTS AND DISCUSSION

We study vibrational properties of the MgO clusters, paying more attention to their relationship with the cluster geometrical structures in order to find the cluster specific spectra.

Table 1 above shows the spectra of all types of MgO clusters ranging in size from a few atoms to the bulk, which have three different mode regions at or near, the high frequency cluster vibrations corresponding to stretching modes, intermediate frequency corresponding to combination of stretching mode and bending, and low frequency vibrations corresponding to bending vibrational modes. The IR spectra for the structure of the eight isomers MgO nanotube clusters were investigated as displayed in Fig. 1, and the calculated vibrational frequencies in the IR are collected in Tables 2, 3, 4 and 5. The choice of these clusters is based on our previous analysis on II-VI clusters [8].

Table1. Calculated vibration excitations for MgO and of $(MgO)_n$ (n = 3, 4, 6, 8, 9 and 12) clusters.

System	Structure	High frequency	Intermediate frequency	Low frequency
MgO	Molecule [a]	12.7 µm	–	–
$(MgO)_n$	Cluster [b]	16 µm, broad band	22 µm, broad band	–
MgO	Bulk [b]	–	25 µm, broad band	–
$(MgO)_3$	Hexa- ring	770-792cm^{-1}	267-609 cm^{-1}	164-192 cm^{-1}
$(MgO)_4$	Octa- ring	865-884 cm^{-1}	260-725cm^{-1}	82-196 cm^{-1}
$(MgO)_6$	2-hexa-ring	526-681cm^{-1}	365-522 cm^{-1}	136-325 cm^{-1}
$(MgO)_6$	Slab	568-738 cm^{-1}	297-556 cm^{-1}	219-285 cm^{-1}
$(MgO)_8$	2-octa ring	514-752 cm^{-1}	265-512 cm^{-1}	66-250 cm^{-1}
$(MgO)_9$	3-hexa ring	552-696 cm^{-1}	384-513 cm^{-1}	126-375 cm^{-1}
$(MgO)_9$	Slab	561-705 cm^{-1}	306-455 cm^{-1}	189-289 cm^{-1}
$(MgO)_{12}$	Sphere	706-724 cm^{-1}	344-557 cm^{-1}	106-327 cm^{-1}

[a] Ref [15]
[b] Taken from Ref [26]

Table 2. Frequencies and intensities of the infrared modes of $(MgO)_n$, n = 3 and 4.

Mode	Frequency /cm^{-1}	IR-Intensity /km.mol^{-1}	Mode	Frequency /cm^{-1}	IR-Intensity /km.mol^{-1}
(a) $(MgO)_3$ (hexagonal ring stack)					
1A˝	163.8532	0.0011	7A´	526.4732	0.0000
2A´	165.7923	0.0082	8A˝	608.3977	2.3476
3A˝	190.9752	76.4822	9A´	609.2354	2.1387
4A´	191.8962	76.3621	10A˝	768.3721	273.4456
5A´	266.8205	216.6842	11A´	769.9084	274.8274
6A´	358.8431	0.0000	12A˝	792.8201	0.0328
(b) $(MgO)_4$ (octagonal ring stack)					
$1B_{1u}$	82.0567	0.0000	$10A_{1g}$	296.1164	0.0000
$2B_{2g}$	101.6276	0.0000	$11A_{1g}$	440.9143	0.0000
$3B_{1g}$	103.3844	0.0000	$12E_u$	531.9645	4.9401
$4B_{2u}$	110.8741	0.0000	$13E_u$	531.9623	4.9401
$5E_g$	195.9994	0.0000	$14B_{2g}$	724.5007	0.0000
$6E_g$	195.9994	0.0000	$15B_{1g}$	724.7566	0.0000
$7E_u$	228.7521	150.4347	$16E_u$	864.9365	381.3476
$8E_u$	228.7521	150.4336	$17E_u$	864.9354	381.3461
$9A_{2u}$	259.6312	304.8842	$18A_{2g}$	883.7723	0.0000

Table 3. Frequencies and intensities of the infrared modes of $(MgO)_6$ cluster.

Mode	Frequency /cm^{-1}	IR-Intensity /km.mol^{-1}	Mode	Frequency /cm^{-1}	IR-Intensity /km.mol^{-1}
(a) $(MgO)_6$ (2-hexagonal ring stack)					
1A´	136.3512	0.0000	16A˝	436.3256	0.0005
2A˝	140.1645	0.0000	17A´	437.1927	2.3476
3A	204.4152	33.0922	18A´	444.1259	0.0017
4A	204.4670	32.1461	19A´	496.6784	0.0302
5A´	264.0209	28.5702	20A˝	520.5087	18.2940
6A´	279.3343	0.0000	21A´	521.8255	22.7287
7A˝	280.2983	1.0000	22A´	526.1367	653.4918
8A˝	318.0476	0.0000	23A´	560.5621	0.0010

9A˝	325.9508	0.0004	24A˝	560.6924	0.0004
10A′	365.1587	107.9652	25A˝	638.5023	0.1439
11A˝	365.3932	109.4721	26A′	639.4536	0.1407
12A′	398.8245	0.0007	27A˝	641.2435	0.0053
13A˝	409.9734	0.0032	28A˝	675.1786	3.6921
14A˝	410.0941	0.0841	29A˝	678.2365	577.3264
15A˝	429.5997	1.0763	30A′	680.8249	582.5510
(b) $(MgO)_6$ (slab structure)					
$1A_2$	218.5202	0.0000	$16A_1$	444.1335	0.0000
$2A_2$	228.0958	0.0000	$17B_2$	457.4942	10.4764
$3B_1$	243.6194	8.8621	$18A_2$	477.3613	0.0000
$4B_2$	253.3698	0.7186	$19A_2$	485.7681	0.0000
$5A_1$	269.5493	0.0000	$20B_1$	512.1819	0.0000
$6B_1$	276.4943	0.0000	$21B_2$	521.7704	0.0000
$7A_1$	285.1326	0.0000	$22A_1$	523.8752	0.0000
$8B_2$	296.8438	96.2136	$23A_1$	555.5883	6.2023
$9B_2$	299.3512	0.0000	$24B_1$	567.9397	503.1312
$10B_1$	315.1534	115.5991	$25A_1$	573.0865	0.0000
$11A_1$	335.5385	11.6542	$26B_2$	581.7945	551.2063
$12A_2$	363.1398	0.0000	$27B_2$	607.0753	0.0000
$13A_1$	420.6883	0.0000	$28A_1$	612.5203	218.0634
$14A_1$	432.5794	158.7798	$29B_1$	703.2945	0.0000
$15B_1$	438.9037	0.1164	$30A_1$	737.5961	488.9604

Table 4. Frequencies and intensities of the infrared modes of $(MgO)_9$ clusters.

Mode	Frequency /cm^{-1}	IR-Intensity /$km.mol^{-1}$	Mode	Frequency /$km.mol^{-1}$	IR-Intensity /cm^{-1}
(a) $(MgO)_9$ (3-hexagonal ring stack)					
$1B_1$	125.5321	14.2070	$25B_2$	435.8946	45.5386
$2A_1$	128.1291	14.2003	$26B_1$	435.9761	9.8542
$3A_2$	183.7058	0.0000	$27A_1$	440.5495	8.0961
$4B_2$	185.8709	0.0000	$28A_1$	441.1784	3.8309
$5A_1$	228.6320	0.3577	$29B_1$	444.2453	15.1496
$6A_2$	236.3523	0.0000	$30A_2$	482.0154	0.0000
$7A_2$	237.5087	0.0000	$31B_2$	482.8952	0.0043
$8B_2$	238.7671	0.0000	$32B_1$	505.4276	36.8177
$9A_1$	244.8554	0.0614	$33A_1$	510.9407	36.4465
$10B_1$	257.4844	0.0832	$34A_1$	513.4798	4.3123
$11A_1$	258.4023	0.1213	$35A_2$	542.5791	0.0000
$12B_1$	276.1546	8.7439	$36B_2$	547.6822	0.9325
$13A_1$	280.0312	9.1932	$37B_2$	551.8895	361.6266
$14B_1$	297.0041	24.2351	$38B_1$	559.6832	46.1892
$15A_1$	299.0756	25.9972	$39A_1$	563.3165	57.7034
$16B_2$	316.1876	3.7684	$40A_2$	614.6323	0.0000
$17A_2$	343.6551	0.0000	$41B_2$	615.7508	0.0121
$18B_2$	344.0153	0.0042	$42A_2$	663.7113	0.0000
$19B_1$	364.1065	2.0650	$43B_1$	666.5004	66.0589
$20A_1$	375.0561	0.2268	$44B_1$	674.7557	616.2764
$21B_1$	383.8942	218.2276	$45A_1$	679.4175	684.6588
$22A_1$	386.6724	211.6959	$46A_2$	689.6243	0.0000
$23B_2$	393.6164	229.2071	$47B_2$	693.2194	15.3275
$24A_1$	406.8840	0.0000	$48B_2$	696.0631	700.2484
(b) $(MgO)_9$ (slab structure)					
$1B_1$	189.9954	0.0000	25E	402.8476	58.0894
$2B_2$	192.9376	0.0000	$26B_1$	411.2556	0.0000
$3A_1$	203.2189	1.6598	$27A_1$	428.7063	31.4632

$4A_1$	222.0427	0.0145	28E	431.6962	241.6468
$5B_1$	223.4546	0.0000	29E	431.6974	241.6477
6E	231.6752	0.0584	$30A_1$	455.1813	31.6805
7E	231.6753	0.0585	$31B_1$	490.1859	0.0000
$8B_2$	247.7448	0.0000	32E	494.6961	0.0041
9E	251.7621	7.6834	33E	494.6964	0.0041
10E	251.7624	7.6837	$34A_2$	525.9743	0.0000
$11B_1$	261.011	0.0000	$35A_1$	542.1553	8.7485
$12A_2$	288.7286	0.0000	$36B_2$	544.3696	0.0000
13E	299.3642	0.3809	37E	561.4593	127.7204
14E	299.3648	0.3809	38E	561.4590	127.7204
$15A_1$	306.1772	205.0298	39E	592.3135	119.6384
$16B_1$	313.2078	0.0000	40E	592.3135	119.6385
17E	338.4557	0.6653	$41A_1$	605.9554	576.3579
18E	338.4567	0.0042	$42B_2$	608.8275	0.0000
19E	365.3589	2.7115	43E	628.3614	98.9406
20E	365.3589	2.7115	44E	628.3615	98.9406
$21A_1$	375.7462	21.8872	$45A_2$	636.6022	0.0000
$22B_2$	379.9864	0.0000	46E	705.3806	646.0567
$23A_1$	398.0843	20.6981	47E	705.3812	646.0523
24E	402.8478	58.0905	$48B_2$	710.2084	0.0000

Table 5. Frequencies and intensities of the infrared modes of the $(MgO)_n$ (n = 8 and 12) clusters.

Mode	Frequency /cm^{-1}	IR-Intensity /$km.mol^{-1}$	Mode	Frequency /cm^{-1}	IR-Intensity /$km.mol^{-1}$
(a) $(MgO)_8$ (2-octagonal ring stack)					
$1B_1$	65.7074	0.0000	$22B_1$	401.8809	0.0000
$2B_2$	74.0846	0.0000	$23B_2$	407.4702	0.0000
$3B_1$	135.4285	0.0000	$24A_1$	432.1143	0.2284
$4B_2$	141.0001	0.0000	25E	435.8302	0.2357
5E	164.7905	0.2330	26E	435.8302	0.2356
6E	164.7905	0.2330	$27A_1$	470.8123	0.4194
$7A_1$	223.0135	34.2307	28E	477.4460	29.2357
8E	250.0312	0.3864	29E	477.4461	29.2357
9E	250.0312	0.3863	$30A_1$	512.7407	90.6193
10E	265.0789	71.9005	31E	513.7123	0.0318
11E	265.0789	71.9005	32E	513.7126	593.2346
$12A_1$	291.9705	0.0243	$33B_1$	593.234	0.0000
$13B_1$	306.7078	0.0000	$34B_2$	594.0436	0.0000
$14B_2$	308.2664	0.0000	$35B_1$	672.0392	0.0000
$15A_2$	329.0012	0.0000	$36B_2$	676.7002	0.0000
$16A_1$	345.7183	0.4846	37E	721.6412	1.1146
$17A_1$	355.31005	0.0032	38E	721.6413	1.1146
18E	377.8577	55.4203	$39A_2$	724.3326	0.0000
19E	377.8575	55.4203	40E	752.3824	778.4532
20E	387.8038	123.5744	41E	752.3824	778.4522
21E	387.8038	123.5744	$42A_2$	754.8332	0.0000
(b) $(MgO)_{12}$ (sphere)					
$1T_g$	105.8645	0.0000	$34T_g$	433.4722	0.0000
$2T_g$	105.8645	0.0000	$35T_g$	433.4722	0.0000
$3T_g$	105.8645	0.0000	$36T_g$	433.4722	0.0000
$4E_g$	147.9078	0.0000	$37A_g$	477.0642	0.0000
$5E_g$	147.9078	0.0000	$38E_u$	481.8312	0.0000
$6E_u$	156.7123	0.0000	$39E_u$	481.8312	0.0000
$7E_u$	156.7123	0.0000	$40T_g$	488.3997	0.0000

$8T_u$	159.6976	11.5345	$41T_g$	488.3997	0.0000
$9T_u$	159.6976	11.5345	$42T_g$	488.3997	0.0000
$10T_u$	159.6976	11.5345	$43A_u$	505.8721	0.0000
$11T_u$	166.0468	7.8556	$44E_g$	524.5243	0.0000
$12T_u$	166.0468	7.8556	$45E_g$	524.5243	0.0000
$13T_u$	166.0468	7.8556	$46T_u$	541.4265	134.6975
$14T_u$	194.5347	0.0000	$47T_u$	541.4265	134.6975
$15T_g$	194.5347	0.0000	$48T_u$	541.4265	134.6975
$16T_g$	194.5347	0.0000	$49T_u$	556.6944	83.2345
$17T_u$	247.4089	32.3264	$50T_u$	556.6944	83.2345
$18T_u$	247.4089	32.3264	$51T_u$	556.6944	83.2345
$19T_u$	247.4089	32.3264	$52T_g$	590.1829	0.0000
$20T_g$	272.0693	0.0000	$53T_g$	590.1829	0.0000
$21T_g$	272.0693	0.0000	$54T_g$	590.1829	0.0000
$22T_g$	272.0693	0.0000	$55T_g$	663.4055	0.0000
$23E_g$	314.6969	0.0000	$56T_g$	663.4055	0.0000
$24E_g$	314.6969	0.0000	$57T_g$	663.4050	0.0000
$25A_g$	322.0134	0.0000	$58T_u$	706.1976	225.6388
$26A_g$	327.2265	0.0000	$59T_u$	706.1976	225.6388
$27T_g$	344.1525	145.3944	$60T_u$	706.1976	225.6388
$28T_g$	344.1525	145.3944	$61T_u$	724.0915	766.8125
$29T_g$	344.1525	145.3944	$62T_u$	724.0915	766.8125
$30A_g$	351.1753	0.0000	$63T_u$	724.0915	766.8125
$31T_u$	402.8754	151.5396	$64E_g$	732.5571	0.0000
$32T_u$	402.8754	151.5396	$65E_g$	732.5571	0.0000
$33T_u$	402.8754	151.5396	$66A_g$	737.1259	0.0000

As shown in Fig. 2, the two different isomers of $(MgO)_6$, and $(MgO)_9$ clusters, have remarkably different spectra, from which it is clearly seen that each cluster has its own vibrational frequencies, which sensitive to structures and bonding. The infrared spectral region exhibits three dominant regions, which covered a wide wavelengths range, and each region reveals a number of vibration modes.

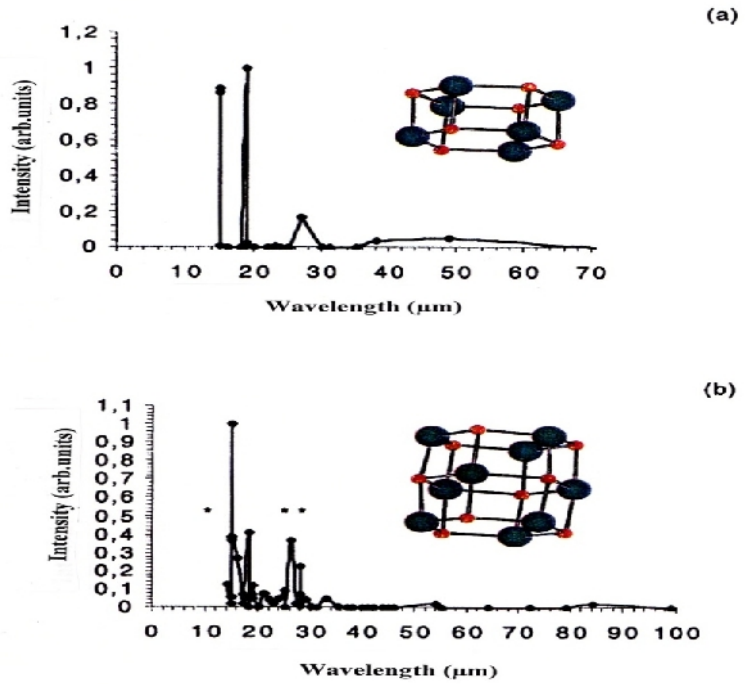

Fig. 2.Vibrational spectra of $(MgO)_n$ clusters shown in Figure 1, **(a)** IR spectra of $(MgO)_6$ cluster, the IR spectrum shows the presence of two features, one located at 14.7 μm and one at 18.7 μm, **(b)** $(MgO)_9$ shows the presence of one clear peak at 14.6 μm. Asterisks (*) and (**) mark the experimental values of MgO molecule and bulk vibration modes respectively.

The most intense feature appearing at around 526 cm^{-1} (19 µm), also there are two main modes have found at roughly 678 cm^{-1} (14.7 µm) and 681 cm^{-1} (14.6 µm), taking this to represent the fundamental of highest frequency. With its intensity is significantly lower corresponding to weak sharp peak at 365 cm^{-1} (27.3 µm), were observed, plus a broad bands only from 264 to 204 cm^{-1} (34 to 64 µm) contain additional weak and special peaks at 264 and 204 cm^{-1} in the low frequency region. The predicted spectra at high and intermediate energy identified for $(MgO)_9$ cluster is shown in Fig. 2(b).

The calculations show, four intense peaks in the high frequency region, 679 cm^{-1} (14.7 µm), 674 cm^{-1} (14.8 µm), 552 cm^{-1} (18.1 µm), with one distinct peak at 696 cm^{-1} (14.4 µm) as the first strongest vibrational mode, which considerably much more intense than the other three. Interestingly, it consists of broad features found in the intermediate energy region from ca. 394-384 cm^{-1}. In addition, it is noteworthy that the calculations reveal also two additional features located at 299 and 297 cm^{-1}. These results are fully consistent with the experimental 16-22µm, applied IR-REMPI spectra technique [26], and also found to be agreement with the density functional theory [20].

I. ***A. (MgO)$_{3,4}$ Clusters***

The vibrational mode frequency for $(MgO)_3$ and $(MgO)_4$ clusters is shown in (Tables 2). We start with $(MgO)_3$, it exhibits only two vibrations of A′ symmetry are at 267 and 770 cm^{-1}, and the A″ mode is at a frequency of 768 cm^{-1}. Their IR intensities are 217, 275 and 273 km mol^{-1} respectively. However, in the $(MgO)_4$ case, the energy is higher and shows rather different modes such as $A_{1g,}$ $A_{2g,}$ A_{2u}, B_{1g}, B_{2g}, B_{1u}, B_{2u}, E_g and E_u, have only IR activities at E_u, A_{2u} and E_u modes at 865, 260 and 229 cm^{-1} respectively. On the other hand, no new vibrational mode with strong intensity was observed, and most of the $(MgO)_4$ characteristic mode vibrations remain at the same high and intermediate frequencies as for $(MgO)_3$ cluster.

II. ***B. (MgO)$_{6,9}$ Clusters***

There are two different stable structures for the $(MgO)_6$ and $(MgO)_9$ clusters. Their geometry and mode frequency are shown in Fig.1 and (Table 3 and 4) respectively. As the cluster size increases, the additional modes appear for n = 6 and 9. When n = 6, both models consist of a 2-six-membered ring being either in a hexagonal ring stack or slab structure having almost the same energies. The vibrational modes of both structures are very similar, that have three intensive modes at A′ (681 cm^{-1}), A″ (678 cm^{-1}), A′ (526 cm^{-1}) and A_1 (738 cm^{-1}), B_2 (582 cm^{-1}) and B_1 (568 cm^{-1}) for 2-hexagonal ring and slab structure respectively. Similarly, we found for n = 9 that there are four identified IR active modes at 696 cm^{-1} (B_2), 679 cm^{-1} (A_1), 675 cm^{-1} (B_1) and 552 cm^{-1} (B_2) for 3-hexagonal ring stack while, 705.3812 cm^{-1}, 705.3806 cm^{-1} have assigned to the E modes, and 606 cm^{-1} has assigned to the A_1 mode for slab structure. The activity of the IR modes in 3-hexagonal ring stack here is similar to slab structure which has the same layers with different in models (see Table 4). Motions in these clusters are results in IR active modes due to Mg−O stretching modes.

III. ***C. (MgO)$_{8,12}$ Clusters***

As the clusters grow in size even more, gave rise to appear a new mode and however, increase in the intensity. For $(MgO)_8$, there are five modes representation, $A_{1,}$ $A_{2,}$ B_1, B_2 and E. This is reveals only one active mode vibration A_1 symmetry at 513 cm^{-1} and also has the E modes, seem to be lamped to one intensive mode of frequency 752 cm^{-1}. Whereas, in the case of $(MgO)_{12}$, it contains A_g, $A_{u,}$ E_g, E_u, T_g and T_u. All IR activities have a new characteristic mode symmetry of T_u, which contain three modes seem to emerge in one extensive mode at T_u (724 cm^{-1}), and three modes gathering in one less intense at T_u (706 cm^{-1}). As in the case of $(MgO)_8$ and $(MgO)_{12}$, motion in these structures gives rise to strong IR modes.

On the other hand, due to the exceptional properties of MgO clusters, these materials exhibit a new optical storage media with high transparent. The initial concept based on the optical transmittance and making adequate buffer layer in MgO materials, that satisfied the requirements for transparent bodies to reduce summer time radiant heat from windows especially in buildings, automobile, trains, and other industry areas.

IV. CONCLUSION

The Infrared spectra of eight isomers, hexagonal ring $(MgO)_3$, octagonal ring $(MgO)_4$, 2-hexagonal ring stack and slab structure $(MgO)_6$, 2-octagonal ring stack $(MgO)_{8,}$ 3-hexagonal ring stack and slab structure $(MgO)_9$ and spherical cluster $(MgO)_{12}$ have been studied computationally at the density functional B3LYP/6-311G (d).

The main results of this work lead us to the following conclusions:

(i) The wavelength spectra of nanoparticles $(MgO)_3$, $(MgO)_4$, $(MgO)_6$, $(MgO)_8$, $(MgO)_9$, and $(MgO)_{12}$ clusters studied have three different regions at high frequency, intermediate frequency and low frequency, covered a wide wavelengths rang, and each region vibrating in different IR frequency range. The maximum intensity is increasing or decreasing with cluster size change and the number of optically active modes is estimated.

(ii) The motion in these clusters gives rise to show characteristic active modes corresponding to all clusters and change noticeably as they change from $(MgO)_3$ to $(MgO)_{12}$ cluster structures.

For small clusters, n = 3 and 4, both have a single intense at 770 and 865 cm^{-1}, while for the larger clusters, n = 6, three intensive modes are observed in the longer wavelength region at 526, 678, 681 cm^{-1} and 567, 582, 738 cm^{-1} for hexagonal ring staked and slab structure respectively. For n = 9, the most intense frequencies, located at 696, 679, and 675 cm^{-1} for 3-hexagonal ring stacked whereas, one intensive mode at 705 cm^{-1} and another interesting feature at 606 cm^{-1} for slab structure.

The infrared spectra of $(MgO)_8$ is determined by two strong single intense at 752 cm^{-1} and 514 cm^{-1} with weaker intensity at 388 cm^{-1}, while, the spectrum of $(MgO)_{12}$, three modes seems to be emerged in one extremely intense at 724 as an active mode with some features at 706, 557 and 541 cm^{-1}.

We therefore conclude that the highest intensive modes of eight clusters have been identified in the range 525 to 865 cm^{-1}.

(iii) MgO materials exhibit transparency medium. This character makes it an ideal candidate for optical technology purposes.

ACKNOWLEDGEMENT

The computing facilities at the Department of Inorganic Chemistry, Gothenburg University, Sweden are acknowledged for their assistance.

REFERENCES

[1]. J. Zhang and L. Zhang, *Chem. Phys. Lett*., **363**, 293 (2002).

[2]. M. Haertelt, A. Fielicke, G. Meijer, K. Kwapien, M. Sierka and J. Sauer, *Phys. Chem. Chem. Phys*., **14**, 2849 (2012).

[3]. X.F. Duan., Y. Huang, R. Agarwal and C.M. Lieber, *Nature*, **421,** 241 (2003).

[4]. C.F. Bohren. and D.R. Huffman, *Absorption and Scattering of Light by Small Particles* (Wiley, New York, 1998).

[5]. G.E. Brown, V.E. Henrich and W. H. Casey et al, *Chem. Rev*. **99**, 77 (1999).

[6]. P.A. Cox and A.A. Williams, *J. Electron Spectrosc. Relat. Phenom*, **39**, 45 (1986).

[7]. A. Fujishima and K. Honda, Electrochemical Photolysis of Water at a Semiconductor Electrode, *Nature* **238**, 37 (1972).

[8]. F. Bawa and I. Panas, *Phys. Chem. Chem. Phys*., **4**, 103 (2002).

[9]. M. Gutowski, P. Skurski, X. Li and L.S. Wang, *Phys. Rev. Lett*., **85**, 3145 (2000).

[10]. I.S. Altman, P.V. Pikhitsa, M. Choi, H.J. Song, A.G. Nasibulin, and E. I. Kauppinen, *Phys. Rev. B* **68**, 125324 (2003).

[11]. W.F. Schneider., L. Ij and C. K. Hass, *J. Phys. Chem. B*,**105**, 6972 (2001).

[12]. F.H. Bawa, *J. Chem. Soc. Pak*. **32**, 319 (2010).

[13]. F.H. Bawa and A. H. Bawa, *J. Chem. Soc. Pak*., **34**, 775 (2012).

[14]. A.M. Vasilevskii, V. A. Volpyas, A.B. Kozyrev and G. A. Konoplev, *Tech. Phys. Lett.*, **34**, 561 (2008).

[15]. K.P. Huber, G. Herzberg, *Molecular Spectra and Molecular Structure, IV, Constant of Diatomic Molecules* (V.N. Reinhold, New York, 1979).

[16]. R.C. Whited, J.F. Christopher and W. C. Walker, *Solid State Comm*. **13**, 1903 (1973).

[17]. S. Hiyoshi, N. Nakamori, J. Hirono and H. Kanamori, *J. Phys. Soc. Jpn*., **43**, 2006 (1977).

[18]. I. Kiyoshi, T. Takuma and K. Aira, *J. Eur. Ceram. Soc*., **26**, 639 (2006).

[19]. V. Pokropivny, *Int. J. Nanotechnol*. **1**, 170 (2004).

[20]. L. Chen, C. Xu, and X.F. Zhang, *J. Mol. Structure (Theochem)* **863**, 55 (2008).

[21]. R.W.G. Wyckoff. *Crystal Structures*, (Wiley, New York, 1963).

[22]. A.D. Becke, *J. Chem. Phys*. **98**, 5648 (1993).

[23]. C. Lee, W. Yang and R. G. Parr, *Phys. Rev. B* **37**, 785 (1988).

[24]. S.H. Vosko, L. Wilks and M. Nusair, *Can. J. Phys.* **58**, 1200 (1988).

[25]. M.J. Frisch, G. W. Trucks and H. B. Schlegel, et al., (*Gaussian* 98, Gaussian Inc., *Pittsburgh* PA, 1998).

[26]. D.V. Heijnsbergen, G.V. Helden, G. Meijer, and M. A. Duncan, *J. Chem. Phys.* **116**, 2400 (2002).